CATEGORY 1

REGULATORY INFORMATION DISTRIBUTION SYSTEM (RIDS)

ACCESSION NBR:9711210060 DOC.DATE: 97/11/13 NOTARIZED: YES DOCKET #
FACIL:50-275 Diablo Canyon Nuclear Power Plant, Unit 1, Pacific Ga 05000275
50-323 Diablo Canyon Nuclear Power Plant, Unit 2, Pacific Ga 05000323
AUTH.NAME AUTHOR AFFILIATION
RUEGER,G.M. Pacific Gas & Electric Co.
RECIP.NAME RECIPIENT AFFILIATION
Document Control Branch (Document Control Desk)

See ~~Ref~~ Proposed Change to Tech Specs

SUBJECT: Forwards response to NRC request for addl info on LAR 97-11 re auxiliary saltwater sys piping bypass unreviewed safety question.

DISTRIBUTION CODE: A001D COPIES RECEIVED:LTR 1 ENCL 1 SIZE: 46+65
TITLE: OR Submittal: General Distribution

NOTES:

	RECIPIENT ID CODE/NAME	COPIES LTTR	COPIES ENCL	RECIPIENT ID CODE/NAME	COPIES LTTR	COPIES ENCL
	PD4-2 LA	1	1	PD4-2 PD	1	1
	BLOOM,S	1	1			
INTERNAL:	ACRS	1	1	FILE CENTER 01	1	1
	NRR/DE/ECGB/A	1	1	NRR/DE/EMCB	1	1
	NRR/DRCH/HICB	1	1	NRR/DSSA/SPLB	1	1
	NRR/DSSA/SRXB	1	1	NUDOCS-ABSTRACT	1	1
	OGC/HDS3	1	0			
EXTERNAL:	NOAC	1	1	NRC PDR	1	1

NOTE TO ALL "RIDS" RECIPIENTS:
PLEASE HELP US TO REDUCE WASTE. TO HAVE YOUR NAME OR ORGANIZATION REMOVED FROM DISTRIBUTION LISTS OR REDUCE THE NUMBER OF COPIES RECEIVED BY YOU OR YOUR ORGANIZATION, CONTACT THE DOCUMENT CONTROL DESK (DCD) ON EXTENSION 415-2083

TOTAL NUMBER OF COPIES REQUIRED: LTTR 14 ENCL 13

A T E G O R Y 1 D O C U M E N T

Pacific Gas and Electric Company

245 Market Street, Room 937-N9B
San Francisco, CA 94105
Mailing Address
Mail Code N9B
P.O. Box 770000
San Francisco, CA 94177
415/973-4684 Fax 415/973-2313

Gregory M. Rueger
Senior Vice President and
General Manager
Nuclear Power Generation

November 13, 1997

PG&E Letter DCL-97-191

U.S. Nuclear Regulatory Commission
ATTN: Document Control Desk
Washington, D.C. 20555

Docket No. 50-275, OL-DPR-80
Docket No. 50-323, OL-DPR-82
Diablo Canyon Units 1 and 2
Response to NRC Request for Additional Information on License Amendment Request 97-11, Auxiliary Saltwater System Piping Bypass Unreviewed Safety Question

Dear Commissioners and Staff:

On August 26, 1997, PG&E submitted License Amendment Request (LAR) 97-11 in PG&E Letter DCL-97-150. LAR 97-11 requested NRC review and approval, in accordance with 10 CFR 50.92, of a modification to the Diablo Canyon Power Plant Units 1 and 2 auxiliary saltwater (ASW) system to bypass approximately 800 feet of Unit 1 and 200 feet of Unit 2 Class 1 ASW piping.

In letters dated September 19, 1997, and October 14, 1997, the NRC staff identified additional information required in order for them to complete their review. PG&E responded to the September 19, 1997, letter in PG&E Letter DCL-97-177, dated October 14, 1997. PG&E's response to the October 14, 1997, request for additional information is enclosed. This additional information does not affect the results of the safety evaluation performed for LAR 97-11.

Sincerely,

Gregory M. Rueger

A001

1/1

200046

Subscribed and sworn to before me
this 13th day of November 1997
County of San Luis Obispo
State of California

Amy J. Calloway
Notary Public

Attorneys for Pacific Gas and
Electric Company
Roger J. Peters
Richard F. Locke

Richard F. Locke

cc: Edgar Bailey, DHS
Steven D. Bloom
Ellis W. Merschoff
Kenneth E. Perkins
David L. Proulx
Diablo Distribution

Enclosures

NRC Mechanical Engineering Branch Request for Additional Information on Auxiliary Saltwater System Piping Bypass Project

Question 1

Indicate if the system is required to operate after experiencing Hosgri earthquake ground motion in order to maintain the plant in a safe shutdown condition.

PG&E Response to Question 1

The auxiliary saltwater (ASW) system supplies cooling water to the component cooling water heat exchangers from the ultimate heat sink (the Pacific Ocean) in order to reject heat from primary plant systems. The system is required to operate following the postulated 7.5M Hosgri earthquake in order to maintain the reactor in a safe shutdown condition (i.e., to support residual heat removal operation).

Reference

1-1 FSAR Update 3.7.6, "Seismic Evaluation to Demonstrate Compliance with the Hosgri Earthquake Requirements Utilizing a Dedicated Shutdown Flowpath."

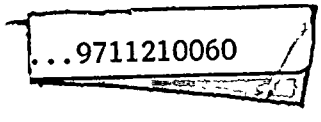

Question 2

Provide detailed justification to demonstrate that the Dresser couplings will function under simultaneous internal pressure and the largest expected dynamic axial displacement.

PG&E Response to Question 2

The Diablo Canyon Power Plant (DCPP) application of the Dresser 24.5 inch, Style 38 coupling requires the ability to withstand cyclic movement of the pipe inside the coupling. Full scale cyclic testing was performed with the pipe "dry" followed by hydrostatic testing at 150 psig. The highest system operating pressure is 102 psig, while the Dresser coupling working pressure specified by the manufacturer is 378 psig. The required displacement for the Hosgri qualification test was 1.5 inches. The maximum displacement requirement for the Hosgri earthquake load combination is calculated as 1.1 inches (Reference 2-1).

During planning stages, PG&E considered cyclic testing with the system internally pressurized with water at 150 psig. This approach was found to be unfeasible because of the high pumping power and numerous other equipment and controls required. The determination was made to do the tests with the pipe dry, and perform hydrostatic tests after the cyclic movement.

The test methods used to qualify the Dresser couplings are considered acceptable for the reasons discussed in the following paragraphs.

Coupling Design:

The pressure retaining design of the coupling does not rely upon internal pressure to seal. The gaskets of the coupling are well confined within the annular space between the follower rings and the middle ring. (See attached sketch of Dresser coupling, Attachment 2-1.) The surface area of the gasket exposed to internal pressure is small. Internal pressure does not result in forces upon the coupling or gaskets that would tend to unseat the gasket or influence the sealing surfaces during displacement.

Potential Failure Mechanisms:

Movement occurs between the pipe surface (Paraline) and gasket. The gasket and middle ring do not move relative to one another. The most likely potential failure mechanism would be "rolling" of the gasket on the pipe disturbing the gasket/middle ring seal. This is prevented by reducing the friction between the Paraline and the gasket to near zero by a lubricant applied to the pipe surface during assembly (Reference 2-2). The potential for chafing or tearing the gasket is similarly reduced by application of the lubricant. The presence of internal pressure is not expected to significantly affect any of these potential failure mechanisms. The function of the seal was not disturbed by cyclic displacements as proven by a hydrostatic test after dynamic tests.

Previous Cyclic Testing Concurrent With Internal Pressure:

Dresser Industries had performed a similar test with a 14 inch, Style 38 coupling in 1978 (Reference 2-3). The two tests cyclically displaced the pipe 1 inch at 10.0 Hz for 30 seconds with an internal pressure of 225 psig. The report noted:

> *"There was no evidence of damage or deterioration to the coupling gaskets as a result of the test as specified in para. 2.0 above with the exception of slight chaffing of the gaskets due to relative motion between the gaskets and piping. The piping section was pressurized to 230 psig during Test 1 and to 240 psig during Test 2. Internal pressure decayed to 195 psig after Test 1 and 190 psig after Test 2. The internal pressure decay may be accounted for by leakage through the regulator There was no visible evidence of water leakage from the coupling during or after the test specified in para. 2.0."*

Based on the results of these tests by Dresser Industries, it is concluded that the presence of internal pressure during cyclic testing would have no important effect on the performance of the coupling, and that the pressure-retaining integrity of the coupling will be maintained.

Hydrostatic Testing and Post-Test Examination of Specimen:

Following the 1996 PG&E cyclic testing, the coupling was subjected to an internal hydrostatic pressure of 150 psig. If there were any damage significant enough to cause leakage, it would be revealed by this test. No leakage or weeping occurred during the hydrostatic test.

The coupling was then disassembled and carefully examined for evidence of damage or deterioration. Some minor pipe Paraline surface scuffing was apparent. However, no other signs of damage or deterioration were observed.

References

2-1 PG&E Letter DCL-97-091, "Response to Request for Additional Information Auxiliary Saltwater System Piping Bypass Project," dated May 15, 1997, Question 8.

2-2 PG&E Letter DCL-97-010, "Auxiliary Saltwater System Piping Bypass Project," dated January 27, 1997, Figure 6.

2-3 Dresser Couplings Seismic Qualifications, Test Report No. 14333, "Seismic Vibration Testing of One 14" Dresser Style 38 Coupling for Dresser Manufacturing Div. of Dresser Industries, Inc. Under Purchase Order No. 37443," dated November 15, 1978 (Attachment 2-2).

Question 3

Provide a copy of the report "Dynamic Soil Properties for Analysis of ASW Piping System Bypass, DCPP," by Robert Pyke, May 28, 1996 (Reference 2, page 25 of Attachment A to the letter of August 26, 1997).

PG&E Response to Question 3

See Attachment 3-1.

Attachment

3-1 Letter from Robert Pyke, Consulting Engineer, to PG&E, dated May 28, 1996, Subject: Dynamic Soil Properties for Analysis of ASW Piping System Bypass, Diablo Canyon Nuclear Power Plant.

Question 4

Provide a detailed discussion of the following statements (page 30 of Attachment A to the letter of August 26, 1997): "The largest calculated soil displacements result from the softest soil (lowest shear velocity), while the internal forces in the buried piping system result from the stiffest soil springs (highest shear wave velocity). To account for variability in input parameters, a conservative combination of spring stiffness and imposed displacement inputs were used in the buried piping model." Show how these were considered in the buried piping calculations.

PG&E Response to Question 4

Design Background

Analysis of the buried piping model is analogous to a beam-on-elastic-foundation problem, except the external forces are applied through the support springs in the form of imposed displacements. Internal equilibrium of the beam-spring model is maintained through opposing spring forces as well as internal forces in the beam elements.

For a given set of support spring stiffnesses, larger input displacements translate into higher externally applied forces. On the other hand, as the support spring stiffness increases, for a given set of input displacements, the beam-spring system behaves similarly to a stiffer structural system subjected to imposed displacement input, resulting in higher internal forces in the beam-spring system.

Parametric Variation of Shear Wave Velocity

Differential displacement input to the buried pipe models is derived from the System for Soil-Structure Interaction (SASSI) site response analyses. To account for variability in the soil properties, parametric variation of shear wave velocities (V_s) using best estimate, lower bound and upper bound values are considered. For a given change in magnitude of V_s relative to the best estimate, it was determined that differential displacements and Winkler spring stiffnesses will vary in the opposite direction by different magnitudes. The results of the parametric studies indicate that a lower bound shear wave velocity gives the largest differential displacements, whereas a higher shear wave velocity translates into stiffer Winkler springs and hence, higher overall stiffness of the spring-beam system.

Table 4-1 shows an example of the parametric study results for the piping segment located between the Intake Structure and Point I as shown on Figure 5b-1 of our response of May 15, 1997 (i.e., same as March 25, 1997 response). This table also shows the sensitivity of differential displacement and the Winkler spring stiffness to changes in shear wave velocity caused by soil property variations. By inspection of this table, the largest relative soil displacement corresponds to the lower bound shear wave velocity, indicative of softer soil, and the largest Winkler spring stiffness corresponds to the upper bound shear wave velocity, indicative of stiffer soil.

Table 4-1

Sensitivity of Differential Displacement and Winkler Spring Stiffness to Changes in Soil Properties (V_s), near Intake Structure.

Case	Maximum Transverse Displacement Relative to Intake Structure (inch)	Winkler Spring Stiffness (k/ft/ft)	Relative Spring Stiffness (normalized to highest values)	Relative Displacement (normalized to highest values)
Upper Bound V_s	0.26	8269	1.00	0.35
Best Estimate V_s	0.61	2227	0.27	0.81
Lower Bound V_s	0.75	844	0.10	1.00

Displacements and Spring Stiffnesses Used in Buried Piping Models

The first pipe segment to be analyzed was from the Intake Structure to Point I as shown on Figure 5b-1 of our response of May 15. 1997 (i.e., same as March 25, 1997 response). Instead of performing several sensitivity studies to determine whether a buried piping model utilizing spring stiffnesses and soil displacements corresponding to the upper bound, best estimate, or lower bound V_s would govern, a more conservative approach was used. This segment was qualified in our calculations using relative displacements based on best-estimate shear wave velocity concurrent with Winkler spring stiffnesses based on upper bound shear wave velocity. Based on Table 4-1, it was judged that this approach was adequate for this segment since the soil displacements imposed would be more than 80 percent of the maximum case (lower bound V_s), while the Winkler spring stiffnesses would be the maximum of the three cases.

To streamline the subsequent analysis efforts for other buried pipe segments, Winkler spring stiffnesses based on upper bound shear wave velocity are used concurrent with relative displacements based on lower bound shear wave velocity in order to very conservatively encompass soil variability effects.

Question 5a

For the buried piping system shown in Figure 5b-1 of your response of March 25, 1997, to an NRC request for information:

a. Provide the detailed basis and calculation of the axial and transverse soil springs stiffnesses.

PG&E Response to Question 5a

Axial Soil Springs

No axial soil springs are used in the buried pipe model since the lateral bending and axial effects are uncoupled as explained in PG&E responses to Questions 5a and 6 in PG&E Letter DCL-97-091, dated May 15, 1997 (i.e., same as March 25, 1997, response). The analysis for lateral bending and axial effects can be uncoupled since all piping segments are straight runs with anchor blocks encasing all pipe bends. The use of several Dresser couplings along the piping system also serves to practically isolate the various segments from one another, and prevents the transfer of axial forces and moments from one segment to an adjacent segment. Evaluation in the axial direction is performed using a manual calculation and conservative application of direction and magnitude of applied friction between the piping and soil in such a manner as to maximize the overall demand.

Transverse Soil Springs for Piping

The stiffness of transverse Winkler springs attached to piping elements, in both the horizontal and vertical directions, is estimated using Equation 7.9 in Ref. 5a-1.

$$k_o = \frac{0.65\, E_s}{1-\nu^2}\left[\frac{E_e\, D^4}{E_b\, I_b}\right]^{\frac{1}{12}}$$

where

D = pipe diameter
E_b = elastic modulus of the pipe
I_b = moment of inertia of the pipe
k_o = Winkler spring coefficient in units of force per unit beam (pipe) length per unit beam (pipe) deflection
E_s = elastic modulus of the soil
E_e = effective elastic modulus of the soil
ν = Poisson's ratio of the soil

Table 5a-1, which summarizes the resulting spring stiffnesses based on upper bound soil properties for various points along the bypass pipe route, and an example calculation for the spring stiffness for Node I are shown below.

Table 5a-1

Winkler Spring Stiffness Calculation at Selected Locations

Node	E_s (1) (ksf)	G (ksf)	Poisson Ratio	E_b (ksf)	I_b ft^4	Dia (ft)	H (depth) (ft)	k_o (k/ft/ft)
A	10982	3922.00	0.4	4.18E+06	0.1014	2	12	7,897
B	11458	4092.00	0.4	4.18E+06	0.1014	2	9	8,269
C	12636	4513.00	0.4	4.18E+06	0.1014	2	6	9,194
D	14451	5161.00	0.4	4.18E+06	0.1014	2	3	10,632
I	12636	4513.00	0.4	4.18E+06	0.1014	2	6.5	9,194
E	11458	4092.00	0.4	4.18E+06	0.1014	2	9	8,269

Note:
(1) $E_s = 2G(1+\nu)$

Sample Winkler Spring Stiffness Calculation for Node I

$$k_o = \frac{0.65\,E_s}{1-\nu^2}\left[\frac{E_e\,D^4}{E_b\,I_b}\right]^{\frac{1}{12}}$$

with effective soil modulus E_e taken as equivalent to E_s,

$$k_o = \frac{0.65\times 12636}{1-0.4^2}\left[\frac{12636\times 2^4}{4.18E6\times 0.1014}\right]^{\frac{1}{12}}$$

$$k_o = 9194\left(\frac{k}{ft}\right)\ per\ ft\ tributary\ pipe\ length$$

Transverse Soil Springs for Thrust Blocks

The stiffness of transverse soil springs attached to concrete thrust blocks is estimated using equations from Reference 5a-2 for an equivalent, rigid, embedded cylindrical foundation that accounts for the embedment effect of the soil as shown below:

- Vertical Direction

$$K_V = \frac{4GR}{(1-\nu)}\left[1+1.28\frac{R}{H}\right]\left[1+\frac{1}{2}\frac{D}{R}\right]\left[1+\left(0.85-0.28\frac{D}{R}\right)\frac{\frac{D}{H}}{1-\frac{D}{H}}\right]$$

- Horizontal Direction

$$K_H = \frac{8GR}{(2-\nu)}\left[1+\frac{1}{2}\frac{R}{H}\right]\left[1+\frac{2}{3}\frac{D}{R}\right]\left[1+\frac{5}{4}\frac{D}{H}\right]$$

where

G = shear modulus of the soil

ν = Poisson's ratio of the soil

R = equivalent radius of the anchor (see Diagram 5a-1 below)

D = depth of embedment (taken as height of block as shown in Diagram 5a-2)

H = depth to bedrock

Diagram 5a-1

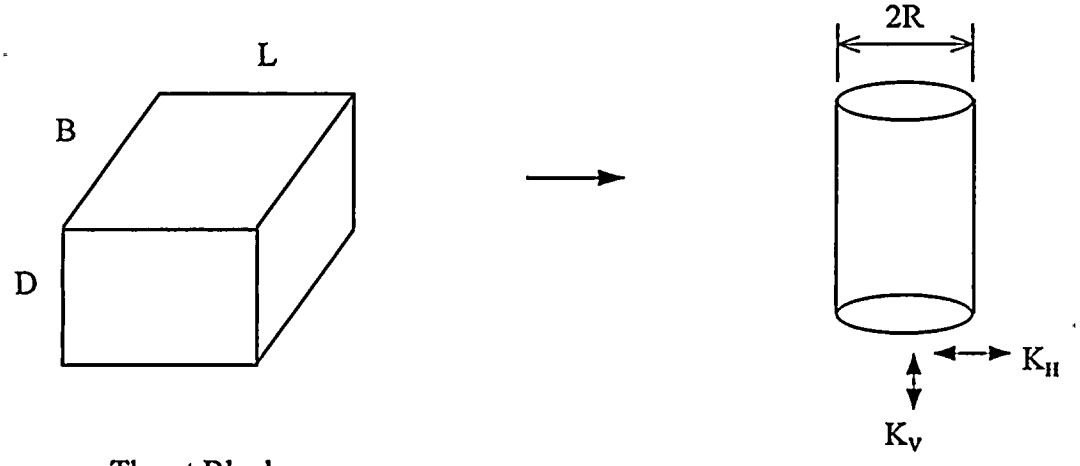

Thrust Block

Equivalent Cylindrical Foundation

Radius, $R = \sqrt{\frac{L \times B}{\pi}}$

Diagram 5a-2

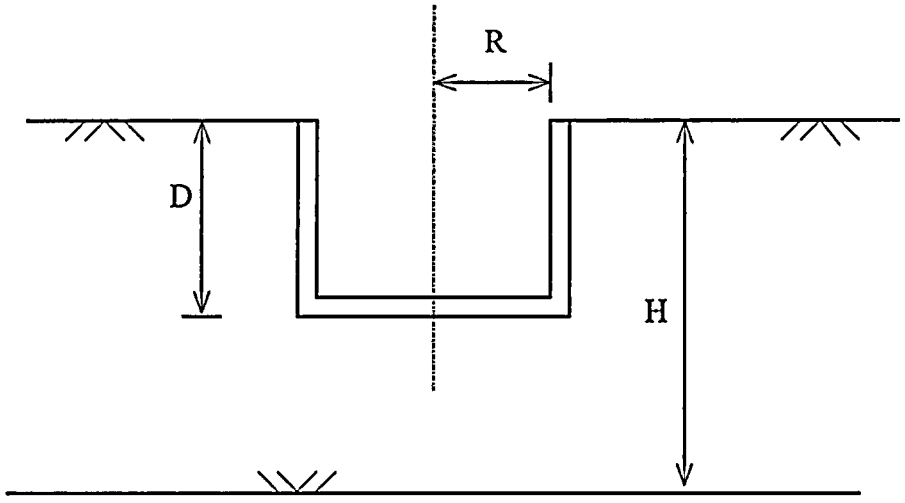

Sample Calculation for Horizontal Soil Spring for Thrust Block E-1

For example, the horizontal soil spring for the thrust block near the Intake Structure, E-1, as shown on Figure 5b-1 of our response of May 15, 1997 (i.e., same as March 25, 1997 response), is calculated as follows:

Thrust Block Dimensions L = 15 ft B = 15 ft D = 10 ft
H = 25 ft
$\nu = 0.4$
G = 4092 ksf

Equivalent Radius, $R = \sqrt{\frac{L \times B}{\pi}}$

$$R = \sqrt{\frac{15' \times 15'}{\pi}} = 8.46\,ft$$

$$K_H = \frac{8GR}{(2-\nu)}\left[1+\frac{1}{2}\frac{R}{H}\right]\left[1+\frac{2}{3}\frac{D}{R}\right]\left[1+\frac{5}{4}\frac{D}{H}\right]$$

$$K_H = \frac{8 \times 4092\,ksf \times 8.46\,ft}{(2-0.4)}\left[1+\frac{1}{2}\frac{8.46\,ft}{25\,ft}\right]\left[1+\frac{2}{3}\frac{10\,ft}{8.46\,ft}\right]\left[1+\frac{5}{4}\frac{10\,ft}{25\,ft}\right]$$

$K_H = 5.43 \times 10^5 \ \frac{k}{ft}$ *for the entire thrust block in the horizontal direction*

References

5a-1 Department of Energy, Seismic Design and Evaluation Guidelines for the Department of Energy High-Level Waste Storage Tanks and Appurtenances, Banyopadhyay, et. al, Brookhaven National Lab., BNL-52361, October 1995.

5a-2 Gazetas, Gary, "Analysis of Machine Foundation Vibrations: State of the Art," published in Soil Dynamics and Earthquake Engineering, Vol. 2, No. 1, January 1983, pp 2 to 42; and associated 1984 errata sheet. (Copy of this reference is attached.)

Question 5b

For the buried piping system shown in Figure 5b-1 of your response of March 25, 1997, to an NRC request for information:

b. Provide the detailed basis and calculation of the frictional forces per unit length acting on the buried piping.

PG&E Response to Question 5b

Friction forces developed at the pipe-soil interface are estimated using Equation 7.4 from Ref. 5a-1. For the general case of a soil possessing both frictional and cohesive strength components, the shear force per unit length of pipe can be estimated from

$$F_{max} = \pi D \left[C_a + \sigma_n \tan(\phi_a)\right]$$

where

$$\sigma_n = \left[\gamma H \frac{(1+K_o)}{2}\right] + \left[\frac{W_p}{\pi D}\right]$$

and

σ_n = average normal pressure between the soil and the pipe due to soil weight, surcharge loading and weight of pipe including its fluid contents

D = pipe diameter; 24 inches

C_a = soil adhesion; considered to be zero since the bypass piping is buried in an envelope of sand

ϕ_a = apparent angle of pipe wall friction; maximum 29° per Table 7.2 of Ref. 5a-1

γ = soil unit weight; 125 pcf for sand envelope/backfill and 150 pcf for reinforced concrete cap slab, where applicable

H = depth of burial, to centerline of pipe

K_o = coefficient of soil pressure at rest; equal to 0.5

W_p = weight of pipe and its fluid contents per foot of pipe; 300 lb/ft

For the buried piping system shown in Figure 5b-1 of our response of May 15, 1997 (i.e., same as March 25, 1997 response), the friction forces at various nodal locations are shown in Table 5b-1 below.

Table 5b-1

Friction Forces at Selected Locations

Node	Depth of Burial (H)		Pipe Weight (W_p) (k/ft)	Diameter (D) (ft)	Normal Soil Stress (σ_n) (ksf)	Friction Force (F_{max}) (k/ft)
	Concrete (ft)	Soil (ft)				
A	0	12	0.3	2	1.17	4.05
B	0	9	0.3	2	0.89	3.08
C	1	5	0.3	2	0.63	2.17
D	1	2	0.3	2	0.35	1.20
I	1	5.5	0.3	2	0.68	2.34
E	0	9	0.3	2	0.89	3.08

Question 5c

For the buried piping system shown in Figure 5b-1 of your response of March 25, 1997, to an NRC request for information:

c. Provide the values of the input displacements to the piping analysis under the following loading conditions:

- **Dead Loads**
- **Soil Settlement Loads**
- **Seismic Loads (HE)**
- **Soil Liquefaction Loads**
- **Tsunami Loads**

PG&E Response to Question 5c

The two primary load contributors for input displacements in the buried piping model are Hosgri earthquake loads and related soil liquefaction loads. The other load contributors are negligible. A discussion of each load contributor is as follows:

Dead Loads:

There are no dead load input displacements in the buried piping model. The effects of dead load on buried piping, especially on flat horizontal piping segments, are minimal due to the continuous support provided by the soil, the relatively small effect from soil surcharge, and off-setting radial ASW operating pipe pressures per References 5c-1 and 5c-2. For instance, considering the maximum burial depth of 12 ft and piping dead weight, the associated external pressure on the piping is approximately 8 psi. Therefore, neglecting the effect of the dead load for the operating ASW pipe under system pressures is conservative.

By judgment, the magnitude of the dead load external pressure on non-operating unpressurized pipe will not affect the integrity of the buried ASW piping.

Soil Settlement Loads:

There are no input displacements associated with the soil settlement loading condition in the buried piping model. Per Reference 5c-3, soil settlement loading is associated with long-term settlement of the underlying soil and bedding material due to gravity and traffic vibrations; and does not include liquefaction-induced settlements. Due to the stringent compaction criteria specified for the underlying soil and bedding material (i.e., relative compaction of 95 percent) as discussed in PG&E response to Question 1 in Reference 5c-4, soil settlement loads are considered insignificant and are neglected.

Hosgri Seismic Loads:

The differential input displacements transverse to the buried piping for the governing Hosgri earthquake are given in Figures 5c-1 through 5c-3. As described in the response to Question 4, input displacements shown in Figure 5c-1 correspond to the best estimate soil properties, while the balance of the bypass piping segments use the more conservative displacement input from lower bound soil properties. In the direction parallel to the piping, the maximum displacements (corresponding to the lower bound V_s) were used for evaluation of the Dresser couplings.

These differential displacement values are derived from the SASSI site response analyses. For a given piping segment, differential displacements are obtained by comparing time history displacement responses at the control locations, such as concrete thrust blocks, to a common reference point.

For a given beam-spring model, internal member forces, especially at the local level, are sensitive to abrupt changes in the direction or magnitude of the input displacements. Abrupt changes in the differential displacement patterns are generally not expected by virtue of (1) the relatively long wave length of the ground motion, i.e., greater than 2,000 feet, compared to the length of the piping segments, and (2) the fact that the soil medium is a continuum with no major physical discontinuities. This is further substantiated by observations of the displacement time histories from the SASSI site response analysis; displacement time histories for control points in a given piping segment are generally in phase with no abrupt direction reversals. Therefore, differential displacements are typically applied using a linear variation between the control points, with the following two exceptions:

(1) Segment between Intake Structure and Point I:

Expected ground movement at the end points of this piping segment is negligible compared to the soil in between since both the Intake Structure and the concrete thrust block at Point I are on bedrock. As shown in Figure 5c-1, differential soil displacement patterns in the transverse directions are conservatively taken as triangular-shaped, with the maximum value at the apex corresponding to the maximum soil displacement relative to the Intake Structure. As far as local stresses are concerned, the triangular pattern selected is more limiting than a more gradual transition, such as a parabola, due to the more abrupt slope change at the apex. For this reason, at points of changing curvature in a given displacement pattern, the more abrupt transition scheme mentioned above, is conservatively applied in lieu of a more gradual transition.

To account for variability in the location of the maximum displacement, the point of application of the maximum displacement is varied ± 8 feet away from the hinge location (Dresser coupling) for this approximate 90 foot-long segment of piping.

(2) Segment between Points D and A:

In the vertical direction (z-direction in Figure 5c-3), review of the displacement time histories at the control points A, C, and D indicates that a direction reversal of displacement pattern may occur at intermediate points between the terminal points at A and D. Conservatively, a triangular displacement pattern with the maximum vertical differential displacement between the terminal points and the "apex" at C is applied. To account for variability, the maximum vertical displacement at C is also applied to C2 in a separate analysis run.

For the horizontal direction, it should be noted that the displacements of one control point relative to another is of primary interest. Therefore, provided the differential displacements between the control points are maintained, the application of maximum displacements at either terminal points A or D would yield the same results.

Soil Liquefaction Loads:

Per Reference 5c-6, the postulated maximum ground settlement near the ground surface associated with the Hosgri earthquake is 0.5 inch. Based on the extent of the liquefiable zone identified in Attachment 1.1 of Reference 5c-4, a vertical displacement pattern as shown in Figures 5c-4 and 5c-5 is used in the buried pipe analysis. These patterns typically impose a maximum vertical settlement value of 0.5 inch within the liquefiable zone, decreasing to zero over approximately 25 feet based on Harding Lawson Associates' recommendation. No concurrent horizontal displacements are specified due to the discontinuous nature of the medium dense sands and the fact that the sands are confined on all sides (Reference 5c-6).

Two piping segments are affected by the liquefiable zone. To account for variability in the size of the liquefiable zone, a total of three analysis runs per segment with varying extent of the maximum settlement zone (0.5 inch) were performed. Liquefaction induced settlement displacements occur at some time following the seismic event due to dissipation of pore pressures in the soil, which are maximized during strong shaking of an earthquake. As a result, the soil spring stiffnesses used in the models are based upon the "at rest" soil properties, rather than the reduced stiffnesses associated with the seismic event.

Tsunami Loads:

There are no input displacements associated with the tsunami loading condition in the buried piping model. Tsunami loads refer to the effect on the buried piping due to the combined effects of tides, storm surge, storm waves, and a tsunami. Storm wave protective measures have been provided to protect the bypass piping from the scouring effects of tsunami conditions. The only tsunami load to be considered is the associated hydrostatic component due to the design basis submergence level over the buried pipes as defined in Reference 5c-5. The maximum hydrostatic pressure for tsunami loading is approximately 12.5 psi and this loading is enveloped by the Hosgri earthquake loading combination.

References

5c-1 PG&E Design Criteria Memorandum M-46, Rev. 23, Piping Pressures, Temperatures and Operating Modes for Unit 1.

5c-2 PG&E Design Criteria Memorandum M-71, Rev. 8, Piping Pressures, Temperatures and Operating Modes for Unit 2.

5c-3 Appendix A to PG&E Design Criteria Memorandum S-17B, Rev. 4, Auxiliary Saltwater System.

5c-4 PG&E Letter DCL-97-177, dated October 14, 1997.

5c-5 PG&E Design Criteria Memorandum T-9, Rev. 2, Wind, Tornado and Tsunami.

5c-6 "Revised Report, Liquefaction Evaluation, Proposed ASW Bypass, DCPP," Harding Lawson Associates, dated August 23, 1996.

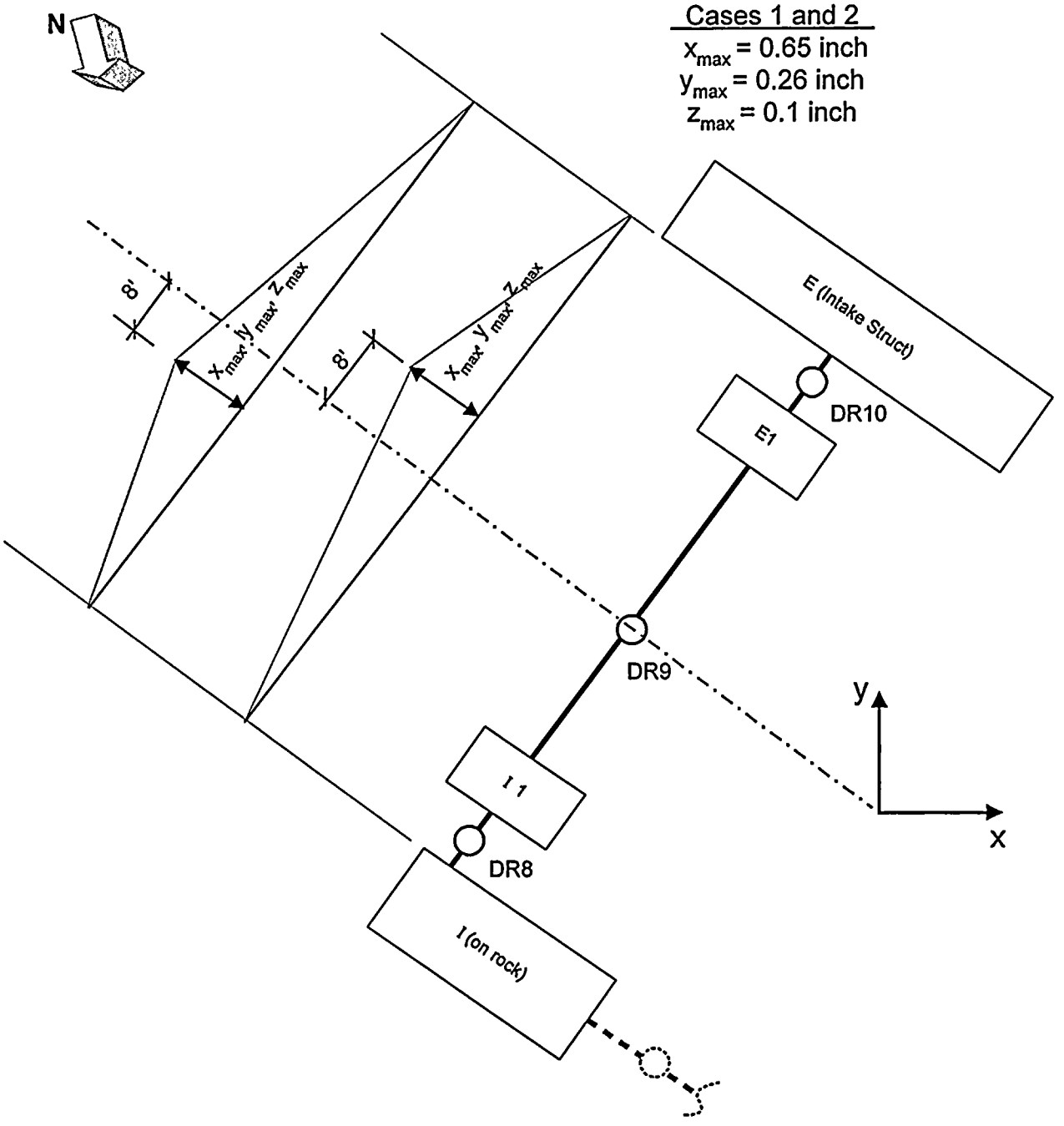

(Not to scale)

Note: Signs are assigned to x_{max} and y_{max} such that the displacements transverse to the pipe are additive.

Figure 5c-1 Hosgri Differential Displacements for Pipe Segment Between E and I

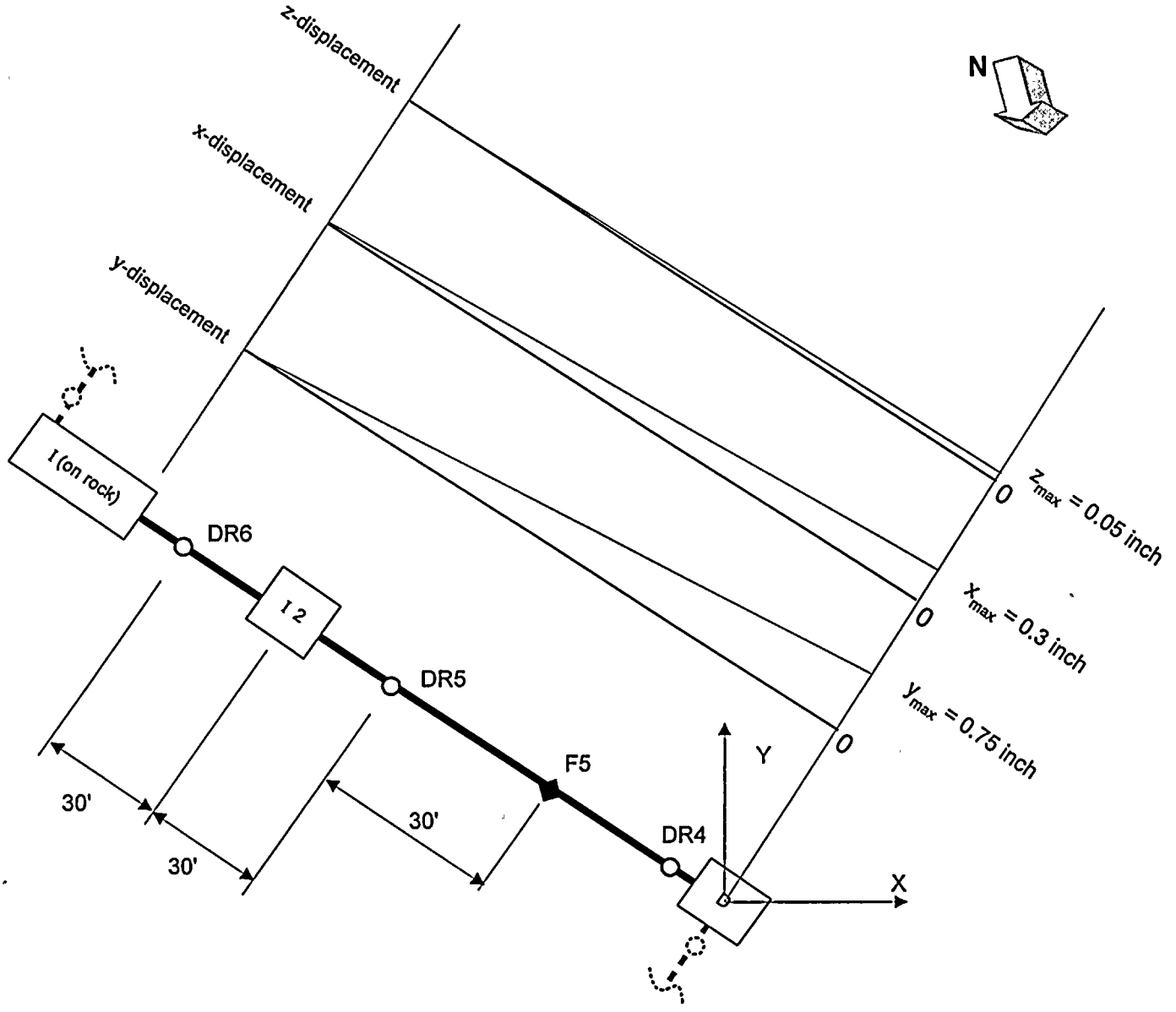

(Not to scale)

Figure 5c-2 Hosgri Differential Displacements for Pipe Segment Between I and D

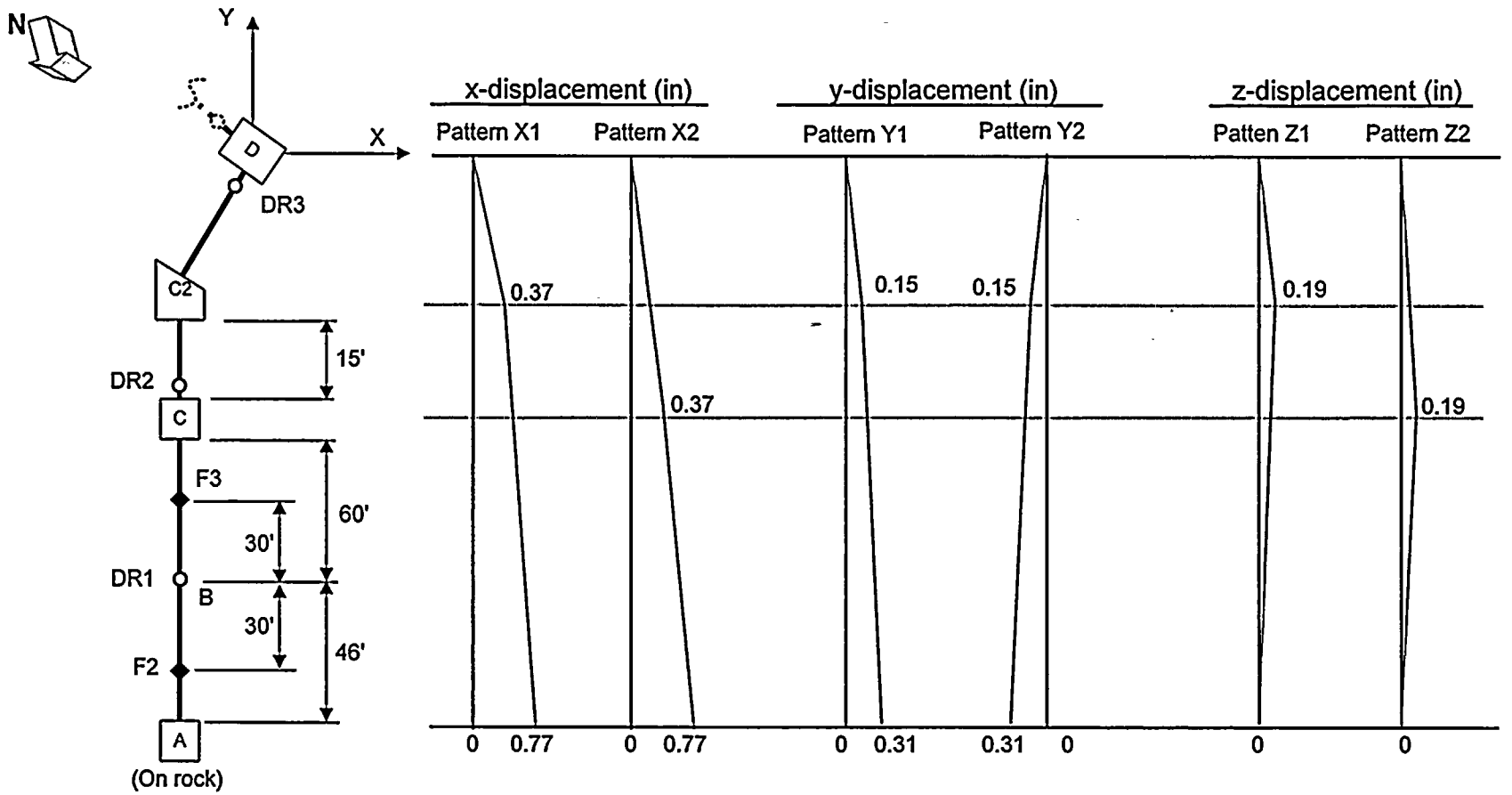

Combination of Displacement Patterns

Case	x-displacement pattern	y-displacement pattern	z-displacement pattern
1	X1	Y1	Z1
2	X2	Y1	Z2
3	X1	Y2	Z1
4	X2	Y2	Z2

Figure 5c-3 Hosgri Differential Displacements for Pipe Segment Between D and A

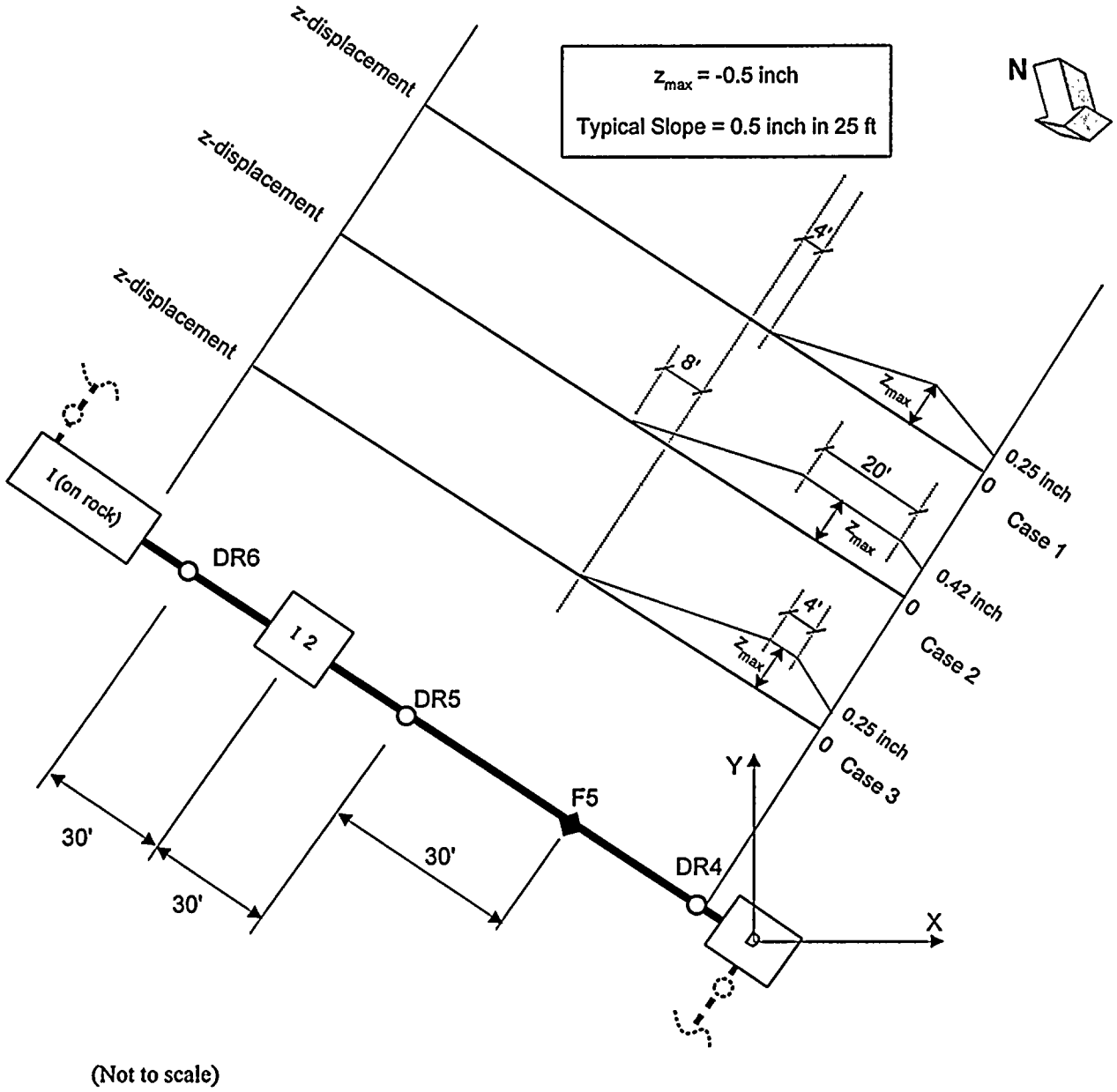

(Not to scale)

Figure 5c-4 Liquefaction Differential Displacements for Pipe Segment Between I and D

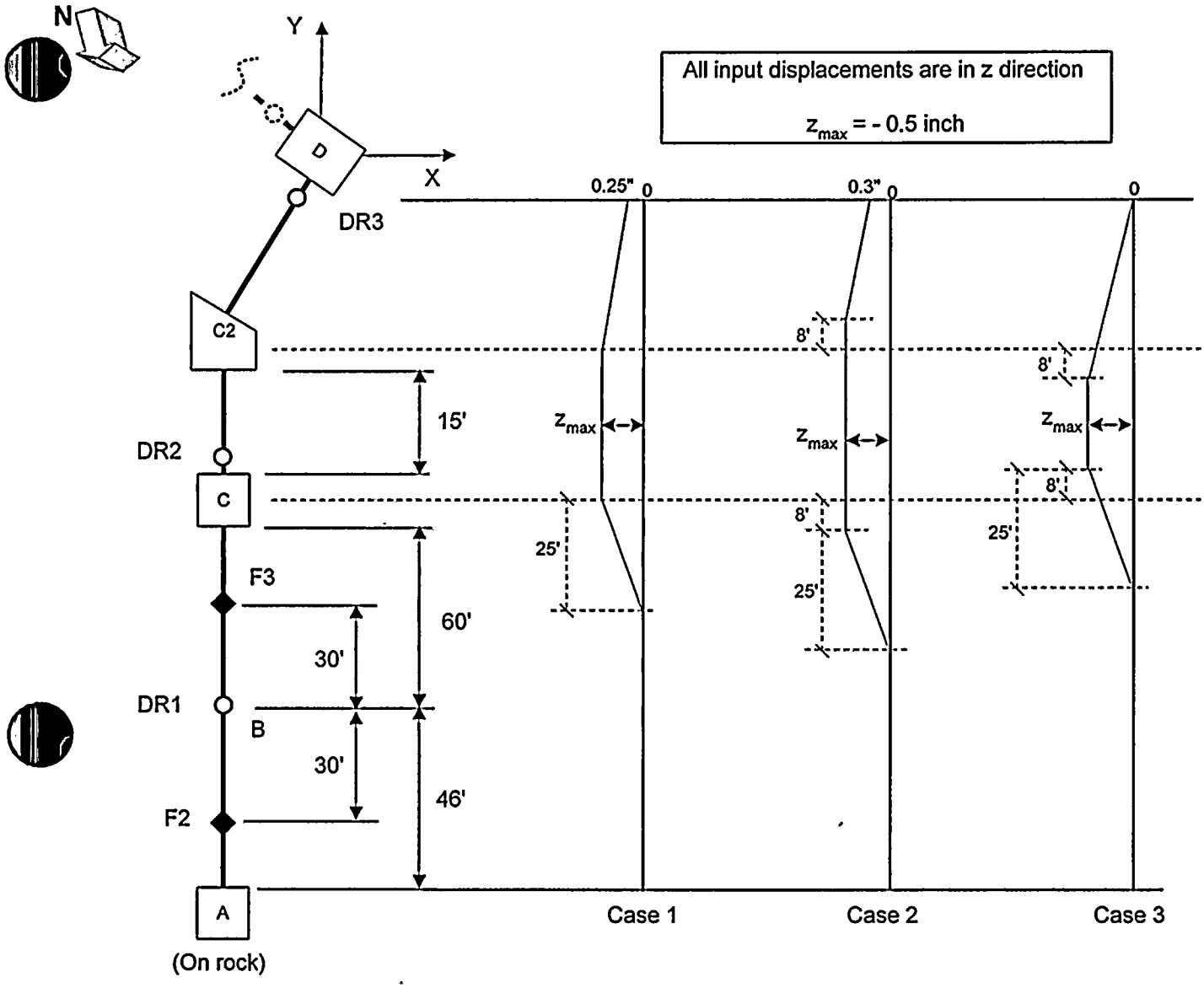

(Not to scale)

Figure 5c-5 Liquefaction Differential Displacements for Pipe Segment Between D and A

Questions 5d & 5f

For the buried piping system shown in Figure 5b-1 of your response of March 25, 1997, to an NRC request for information:

d. Provide the largest design basis demands (axial forces, shear forces, bending moments, torsional moments, displacements and rotations) and their locations on the piping system as a result of the following loading conditions:

- **Dead Loads**
- **Internal Pressure Load**
- **Thermal Loads**
- **Soil Settlement Loads**
- **Seismic Loads (HE)**
- **Soil Liquefaction Loads**
- **Tsunami Loads**

f. Show that the largest pipe stresses resulting from the following load combinations meet the ASW buried piping acceptance criteria:

- **Hosgri Earthquake Combination**
- **Sustained Plus Thermal Load Effect Combination (Soil Settlement Loads and Soil Liquefaction Loads)**
- **Tsunami Combination (considering Soil Liquefaction Loads)**

PG&E Response to Questions 5d and 5 f

Individual Load Components and Controlling Load Combinations

ASW bypass piping is qualified for Hosgri and tsunami design basis events by the following loading combinations per Reference 5c-3:

- Hosgri Earthquake $D + P_A + SS + HE \leq 2.4\ S_h$
- Sustained Plus Thermal Load Effect $D + P_A + T_A + SS + HE \leq (S_h + S_A)$
- Tsunami $D + P_A + SS + TS \leq 2.4\ S_h$

where

D = Dead Load: Includes pipes and equipment, saltwater inside pipes, overlying soils, and any dead load surcharge on the ground surface (including paving, concrete slabs, slope protection materials, and tanks). As discussed in the response to Question 5c, dead load effect is insignificant, and therefore neglected.

P_A = Abnormal Internal Pressure Load: Maximum 102 psi for operating modes per References 5c-1 and 5c-2.

T_A = Abnormal Thermal Load: Induced due to differences in the piping temperature at the time of installation compared to the design temperatures under abnormal conditions. The abnormal temperature range for the ASW piping is associated with ocean temperature and varies from 45 °F to 70 °F.

SS = Soil Settlement Load: Loading on the pipes induced by settlement of the underlying soil and bedding material over time, as a result of gravity and traffic vibrations. Long-term settlement effect is negligible when considering the compaction criteria specified for the underlying soil and bedding material as discussed in response to Question 5c.

HE = Hosgri Earthquake Loading: Input for this seismic loading into the buried piping model is considered at three levels as follows:

1. Analysis of Lateral Effects for Hosgri Event
2. Analysis of Axial Effects for Hosgri Event
3. Hosgri-Induced Liquefaction Effect Following Hosgri Event (LE)

TS = Tsunami Load: Includes the hydrostatic component for a tsunami, which is enveloped by Hosgri loading as discussed in response to Question 5c.

S_h = Allowable material stress at temperature per Reference 5d-1

S_c = Material allowable stress at cold (ambient) temperature per Reference 5d-1

S_A = Material allowable based on 1.25 S_c + 0.25 S_h per Reference 5d-1

Loading combinations for the ASW bypass piping can conservatively be condensed into the following two combinations:

- ~~D~~ + P_A + T_A + ~~SS~~ + HE ≤ 2.4 S_h
- ~~D~~ + P_A + T_A + ~~SS~~ + LE ≤ 2.4 S_h (following Hosgri event)

All ASW bypass piping components, including pipe sections, Dresser couplings, bolted flanges, and concrete thrust blocks are evaluated based on the above loading combinations.

Summary of Results for Pipe Shell and Unencased Flanges

The qualification of ASW bypass pipe shell and unencased flanges per individual segments, as indicated on Figure 5b-1 of our response on May 15, 1997 (i.e, same as March 25, 1997 response), is summarized below:

1. Segment from Intake Structure to Thrust Block I:

Piping Component	Load Component	Maximum Demand on Piping Component
Pipe Shell	HE (max. near mid-span); lateral analysis	M_{33} = 108 k-ft M_{22} = 23 k-ft M_{11} = 0
	HE - friction; axial analysis	P = 99 kips
	T_A - limited by Dresser coupling slip resistance; axial analysis	P = 24 kips
	P_A (102 psi); axial analysis	$\sigma_{PA\ axial}$ = 1.6 ksi $\sigma_{PA\ hoop}$ = 3.2 ksi
	Liquefaction Effect (LE)	Not applicable
Unencased Flanges	No unencased flanges	Not applicable

A. Pipe Shell Evaluations

- $D + P_A + T_A + SS + HE \leq 2.4\ S_h$

$$\sigma_{max} = \frac{P}{A} + \frac{M_r}{Z} + \sigma_{P_A\ axial} \leq 2.4 S_h$$

$$\sigma_{max} = \frac{(99+24)}{27.8\ in^2} + \frac{12 \times \sqrt{(108^2+23^2)}}{162\ in^3} + 1.6\ ksi$$

$$\sigma_{max} = 14\ ksi < 2.4 \times 15\ ksi = 36\ ksi \qquad O.K.$$

- $D + P_A + T_A + SS + LE \leq 2.4\ S_h$

  Not Applicable

B. Unencased Flange Evaluations

No unencased flange in this pipe segment.

2. Segment from Thrust Block I to Thrust Block D:

Piping Component	Load Component	Maximum Demand on Piping Component
Pipe Shell	HE (max. near thrust block at I); lateral analysis	M_{33} = 72 k-ft M_{22} = 7 k-ft M_{11} = 0
	HE - friction; axial analysis	P = 36 kips
	T_A - limited by Dresser coupling slip resistance; axial analysis	P = 24 kips
	P_A (102 psi); axial analysis	$\sigma_{PA\ axial}$ = 1.6 ksi $\sigma_{PA\ hoop}$ = 3.2 ksi
	Liquefaction Effect (LE) (max. near thrust block at D)	M_{33} = 0 k-ft M_{22} = 227 k-ft M_{11} = 0
Unencased 150# Flanges (F5)	HE; lateral analysis	Negligible
	HE - friction; axial analysis	P = 36 kips
	T_A - limited by Dresser coupling slip resistance; axial analysis	P = 24 kips
	P_A (102 psi); axial analysis	$\sigma_{PA\ axial}$ = 1.6 ksi
	Liquefaction Effect (LE) governs	M_{33} = 0 k-ft M_{22} = 113 k-ft M_{11} = 0

A. Pipe Shell Evaluations

- $D + P_A + T_A + SS + HE \leq 2.4\ S_h$

$$\sigma_{max} = \frac{P}{A} + \frac{M_r}{Z} + \sigma_{P_A} \leq 2.4 S_h$$

$$\sigma_{max} = \frac{(36+24)}{27.8\,in^2} + \frac{12 \times \sqrt{(72^2+7^2)}}{162\,in^3} + 1.6\,ksi$$

$$\sigma_{max} = 9.1\,ksi < 2.4 \times 15\,ksi = 36\,ksi \qquad O.K.$$

- $D + P_A + T_A + SS + LE \leq 2.4\ S_h$

$$\sigma_{max} = \frac{P}{A} + \frac{M_r}{Z} + \sigma_{P_A} \leq 2.4 S_h$$

$$\sigma_{max} = \frac{(36+24)}{27.8\,in^2} + \frac{12 \times \sqrt{(227^2)}}{162\,in^3} + 1.6\,ksi$$

$$\sigma_{max} = 20.6\,ksi < 2.4 \times 15\,ksi = 36\,ksi \quad O.K.$$

B. Unencased Flange Evaluation

- $D + P_A + T_A + SS + LE \leq 2.4\ S_h$ (Governs)

  Axial and bending capacities for the 150# flat-faced, weld neck flanges, governed by B7M bolting, are given as:

  $P_{cap} = 270.4$ kips
  $M_{cap} = 388$ k-ft

  P_A has been considered in the development of P_{cap} and M_{cap} given above.
  Using straight line interaction equation for combined loading,

$$IR_{flange} = \frac{P_{max}}{P_{cap}} + \frac{M_{max}}{M_{cap}}$$

$$IR_{flange} = \frac{(24+36)}{270.4} + \frac{113}{388}$$

$$IR_{flange} = 0.51 \quad < \quad 1.0 \quad O.K.$$

3. Segment from Thrust Block D to Thrust Block A:

Piping Component	Load Component	Maximum Demand on Piping Component
Pipe Shell	HE (max. near thrust block at C2); lateral analysis	M_{33} = 53 k-ft M_{22} = 70 k-ft M_{11} = 67 k-ft
	HE - friction; axial analysis	P = 164 kips
	T_A - limited by Dresser coupling slip resistance; axial analysis	P = 24 kips
	P_A (102 psi); axial analysis	$\sigma_{PA\ axial}$ = 1.6 ksi $\sigma_{PA\ hoop}$ = 3.2 ksi
	Liquefaction Effect (LE) (max. near thrust block at C)	M_{33} = 82 k-ft M_{22} = 11 k-ft; M_{11} = small
Unencased 150# Flanges (F2 and F3)	HE; lateral analysis	M_{33} = small M_{22} = small M_{11} = 69 k-ft
	Liquefaction Effect (LE)	M_{33} = 40 k-ft M_{22} = small M_{11} = small

A. Pipe Shell Evaluations

- D + PA + TA + SS + HE ≤ 2.4 Sh

$$\sigma_{max} = \frac{P}{A} + \frac{M_r}{Z} + \sigma_{P_A} \leq 2.4 S_h$$

$$\sigma_{max} = \frac{(164 + 24)}{27.8\ in^2} + \frac{12 \times \sqrt{(53^2 + 70^2 + 67^2)}}{162\ in^3} + 1.6$$

$$\sigma_{max} = 6.8 + 8.2 + 1.6$$

$$\sigma_{max} \approx 16.5\ ksi < 2.4 \times 15\ ksi = 36\ ksi \qquad O.K.$$

- $D + P_A + T_A + SS + LE \leq 2.4\ S_h$

$$\sigma_{max} = \frac{P}{A} + \frac{M_r}{Z} + \sigma_{P_A} \leq 2.4 S_h$$

$$\sigma_{max} = \frac{(164+24)}{27.8\,in^2} + \frac{12 \times \sqrt{(82^2+11^2)}}{162\,in^3} + 1.6\,ksi = 14.5\,ksi < 2.4 \times 15\,ksi = 36\,ksi \quad O.K.$$

B. Unencased Flange Evaluations.

Axial and bending capacities for the 150# flat-faced, weld neck flanges, governed by B7M bolting, are given as:

$P_{cap} = 270.4$ kips
$M_{cap} = 388$ k-ft

P_A has been considered in the development of P_{cap} and M_{cap} given above. Using straight line interaction equation for combined loading, Hosgri loading combination governs:

$$IR_{flange} = \frac{P_{max}}{P_{cap}} + \frac{M_{max}}{M_{cap}}$$

$$IR_{flange} = \frac{(164+24)}{270.4} + \frac{69}{388}$$

$$IR_{flange} = 0.87 < 1.0 \quad O.K.$$

Reference

5d-1 ANSI B31.1, Power Piping, 1973 Summer Addendum

Question 5e

For the buried piping system shown in Figure 5b-1 of your response of March 25, 1997, to an NRC request for information:

e. State if the magnitude of the axial stresses in any load combination was determined from the absolute sum of the axial stresses due to axial effects and the lateral effects. If not, provide justification for not doing so.

PG&E Response to Question 5e

The magnitude of the axial stresses in any load combination was determined from the absolute sum of the axial stresses due to axial effects and the lateral effects. See pipe shell calculations performed in response to Questions 5d and 5f for examples.

Question 6

The load combinations and acceptance criteria that were specified for the Long Term Seismic Program (LTSP) loads are based on EPRI NP-6041. Show that stresses due to load combinations involving LTSP loads meet the licensing basis acceptance criteria for buried piping.

PG&E Response to Question 6

The LTSP margin verification assessment of the ASW bypass piping is not a licensing basis event, but rather a verification of the seismic margin (Reference 6-1). This LTSP margin verification assessment is based on a comparison with the Hosgri results since the Hosgri evaluation is judged to be similar or envelop the LTSP evaluation as explained below.

The horizontal free field spectrum for the 84 percent probability of nonexceedance LTSP is mostly enveloped by the Hosgri free field ground spectrum, as depicted in Figure 3.1 of Reference 6-1. A comparison of horizontal and vertical differential displacements (lower bound soil properties) in Table 6-1 below illustrates that the input displacements to the buried pipe model for the Hosgri and LTSP are not significantly different.

Table 6-1

Comparison of Hosgri and LTSP Differential Displacements

Pipe Segment	Hosgri Differential Displacements		LTSP Differential Displacements	
	Horizontal (in.)	Vertical (in.)	Horizontal (in.)	Vertical (in.)
A-C	0.40	0.19	0.43	0.24
C-D	0.37	0.06	0.39	0.02

Based on inspection of pipe stress evaluations for the Hosgri event shown in response to Questions 5d and 5f, the critical demand stress occurs in the pipe segment from Thrust Block A to Thrust Block D. The maximum stress is 16.5 ksi compared to the allowable stress of 36 ksi for the Hosgri combination. The seismic stress due to the seismic input displacement is approximately 8 ksi. Soil displacements that increase, then decrease along a pipe run, create the largest bending demands in the piping as discussed in the response to Question 5c. Such a condition occurs for the vertical (z direction) displacement in this area (Figure 5c-3). Hence, the larger LTSP seismic demand, principally in the vertical direction, will increase the maximum stress by approximately 2 ksi. There is ample reserve margin available to accommodate the LTSP demand.

References

6-1 NUREG-0675, Supplement 34, Safety Evaluation Report Related to the Operation of Diablo Canyon Nuclear Power Plant, Units 1 and 2, U.S. Nuclear Regulatory Commission, June 1991.

Question 7

State the magnitude of the largest potential aftershock for the Hosgri event. Provide an estimate of the effect on the ASW piping due to the soil and anchor displacements caused by the Hosgri main shock in addition to the ground motion from this aftershock.

PG&E Response to Question 7

In the late 1970s, the maximum magnitude of 7.5 was assessed for the Hosgri fault. The ground motion for this earthquake was developed at the same time and is called the "Hosgri ground motion." The maximum magnitude value of 7.5 for the Hosgri fault has been reviewed and updated in the Long Term Seismic Program (LTSP) Final Report (Reference 7-1) with the revised value of M_w 7.2. To preserve consistency with current scientific thinking, the assessment of magnitude values of potential aftershocks for the Hosgri fault will be referenced to the LTSP results. The Hosgri ground motion, however, still serves as the licensing basis for DCPP.

Aftershock Assessment for a Magnitude 7.2 Earthquake on the Hosgri Fault

As noted in the LTSP Final Report, a conservative evaluation of the maximum magnitude on the Hosgri fault zone at a distance of 4.5 kilometers from the DCPP site was M_w 7.2. The largest aftershock of an earthquake of this magnitude is most likely 1.2 magnitude units less than the mainshock (Reference 7-2). For the mainshock of M 7.2, the largest expected aftershock has a magnitude value of M_w 6.0. The distribution of largest aftershocks reported in Reference 7.2 is a broad, bell-shaped distribution. The likelihood of an aftershock occurring that is close to the same size as the mainshock is small. The larger historical strike-slip earthquakes in California in the San Andreas fault system have had relatively small aftershock sequences. Therefore, a magnitude value of M_w 6.0 is a reasonable value for the largest aftershock associated with the maximum M_w 7.2 event on the Hosgri fault.

Since aftershocks are related to stress adjustments in the crustal rocks in response to the mainshock, areas along the mainshock fault rupture that have experienced the greatest stress release are the areas least likely to release large aftershocks. Most of the aftershock activity would be expected near the ends of the fault rupture. A M_w 7.2 earthquake occurring on the Hosgri fault opposite the plant site would most likely rupture along the segment of the Hosgri fault extending between the northern end of the Hosgri fault north of Point Estero, and the intersection of the Hosgri and Casmalia fault zones near Point Sal (Figure 3-4 of Reference 7-1). The associated fault rupture length is approximately 60 km (Reference 7-3). Therefore, most of the aftershock activity, including the largest aftershock, would be expected to occur near the ends of the fault rupture at a distance of 25 to 35 km away from the plant site. The ground motions expected at the plant site for such an aftershock would be significantly less than those of the mainshock.

Maximum Liquefaction-Induced Vertical Soil Settlement, Including Aftershock Effects

The effect of soil liquefaction on the buried ASW piping has been described in Reference 7-4, under a section entitled "Potential Liquefaction of Soils" (page 20 of Attachment A to Reference 7-4), and in our response to Question 2 of Reference 5c-4. In summary, these liquefaction effects would be limited to only vertical soil settlements acting on buried ASW piping and thrust blocks within the liquefiable soil zone. For a maximum-magnitude Hosgri fault earthquake, conservative upper-bound liquefaction induced vertical soil settlement near the ground surface is estimated to be 0.5 inch. Lateral spreading is precluded because of the limited size of the 5 foot thick liquefiable zone of medium dense sands being surrounded by higher density non-liquefiable materials.

The above vertical settlement values were developed by HLA and are summarized in Reference 5c-6. Per page 5 of Reference 5c-6, HLA addresses the effects of multiple seismic events on liquefaction induced vertical soil settlement estimates as follows:

> *"...While liquefaction has been observed to occur repeatedly at the same site during multiple earthquake, the settlement estimates represent the upper bound of accumulative settlement during repeated events at any given point at the site."(emphasis added)*

Based on HLA's assessment, and considering that the largest Hosgri aftershock is expected to be 1.2 magnitude units smaller than the mainshock and occur at a distance approximately 5 times further away from the site than the main shock, the above vertical settlement values are judged to be maximum values for soil and thrust block displacements for design basis events involving liquefaction, and encompass the combined postulated effect of the Hosgri mainshock and possible multiple aftershocks. The associated buried ASW piping and thrust blocks subject to liquefaction effects have been designed for these maximum vertical settlements as described in our responses to Questions 5c, 5d, 5f, and 8 of this submittal.

Evaluation of Aftershock Effects on the ASW System

The likelihood of an aftershock occurring that is close to the same size as the Hosgri mainshock is small. The ground motions expected at the plant site for an aftershock are significantly less than those associated with the Hosgri mainshock. However, to be conservative in the evaluation of aftershock effects on the ASW system, the following evaluation will assume that the aftershock produces the same level of ground shaking at DCPP as the Hosgri mainshock, concurrent with Hosgri-induced liquefaction settlement effects. The effects of this assumed aftershock shaking on the main components of the ASW system, including buried piping segments, thrust blocks, unencased flanges, and Dresser couplings, are discussed below.

- Pipe Shell

Based on our response to Questions 5d and 5f, the conservative upperbound pipe shell demand stress, regardless of actual demand stress locations, is 35.5 ksi [developed from the summation of the maximum liquefaction-induced demand of 20.6 ksi and the assumed aftershock demand stress (i.e., same as for the Hosgri mainshock) of 16.5 ksi, less the redundant axial stress of 2.5 ksi associated with P_A (1.6 ksi) and T_A (0.9 ksi associated with P =24 kips). This postulated upperbound demand shell stress is less than the allowable 36 ksi for the ASW buried pipe. More realistic stress evaluations of pipe segments within the liquefiable zone are as follows:

Segment from Thrust Block I to Thrust Block D

Based on our response to Questions 5d and 5f, this segment has the maximum liquefaction-induced demand of 20.6 ksi on the pipe shell and this stress is located near Thrust Block D. The assumed aftershock demand stress (i.e., same as for the Hosgri mainshock) for this segment is near Thrust Block I, which is not in the liquefiable zone. This demand stress near Thrust Block D is less than 1 ksi. Therefore, the realistic demand combination near Thrust Block D is approximately 21.6 ksi, which is less than the allowable 36 ksi for the ASW buried pipe.

Segment from Thrust Block D to Thrust Block A

Based on our response to Questions 5d and 5f, this segment has the assumed aftershock demand stress (i.e., same as for the Hosgri mainshock) of 16.5 ksi on the pipe shell and this stress is located near Thrust Block C2. The maximum liquefaction-induced demand stress is 14.5 ksi and is located near Thrust Block C. Note that axial demand stresses due to friction and ASW system pressure are included in both the assumed aftershock and liquefaction-induced demand stresses. Conservatively combining these maximum demands, regardless of the difference in locations, and deducting redundant axial stresses, the maximum demand shell stress for this segment is approximately 23 ksi (i.e., 16.5 ksi + 14.5 ksi - 6.8 ksi - 1.6 ksi), which is less than the allowable 36 ksi for the ASW buried pipe.

- Thrust Blocks

  Based on Table 8-1, the maximum demand moment due to the assumed aftershock (i.e., same as for the Hosgri mainshock) and liquefaction effect for Thrust Block TB-5 is 902 k-ft (i.e., 508 k-ft + 394 k-ft), which is less than the moment capacity of 1,100 k-ft. The associated maximum demand moment due to the assumed aftershock and liquefaction effect for Thrust Block TB-6 is 1,462 k-ft (i.e., 417 k-ft + 1,045 k-ft), which is less than the moment capacity of 1,800 k-ft.

- Unencased 150 Pound Flanges

A total of three unencased flanges are affected by the potential liquefiable zone. Unencased Flanges F2 and F3 are located between Thrust Blocks D and A and unencased Flange F5 is located between Thrust Blocks I and D. As shown in our response to Questions 5d and 5f, the maximum interaction ratio due to the liquefaction effect for the unencased flanges within the liquefiable zone is 0.87 < 1.0, for Flanges F2 and F3. Since the assumed aftershock demands (i.e., same as for the Hosgri mainshock) for the pipe segment between I and D are generally very small, combining the aftershock and liquefaction effects will have a negligible impact on the interaction ratio of the unencased Flange F5. For Flanges F2 and F3, the effect of combining aftershock and liquefaction effect is shown as follows (refer to our response to Question 5d and 5f for demands):

$$IR_{flange} = \frac{P_{max}}{P_{cap}} + \frac{M_{max}}{M_{cap}}$$

$$IR_{flange} = \frac{(164 + 24)}{270.4} + \frac{\sqrt{69^2 + 40^2}}{388}$$

$$IR_{flange} = 0.69 + 0.21 = 0.90 < 1.0 \quad O.K.$$

- Dresser Couplings

As stated in our response to Question 5c, the liquefaction induced ground settlement occurs only in the vertical direction. The effect of the maximum 0.5 inch permanent ground settlement on the Dresser couplings within the potential liquefiable zone includes rotation and axial slip demands. The maximum increase in the rotational demand of the couplings for liquefaction effects is approximately 0.1 degree [i.e., (0.5 inch/25 feet) x (180°/π)]. The maximum increase in axial slip demand for the coupling located on the slope between Blocks C and A is approximately 0.2 inches (i.e., 0.5 inch x sin 23°).

As stated in our response to Question 8 of Reference 7-5, the maximum rotational and axial slip demands for couplings DR1 through DR5 from the Hosgri seismic load combination are 0.02 degrees and 1.1 inches, respectively. These demands are small compared to the allowable rotation of 4 degrees and the tested slip capacity of 2.75 inches [i.e., 2.5 times the maximum displacement demand from Hosgri or LTSP ground shaking (i.e., 2.5 x 1.1. inches)] per our response to Question 9 of Reference 7-5. Therefore, the initial rotation and slip demand at the Dresser coupling due to the liquefaction induced permanent ground settlement has negligible impact on the Dresser couplings within the liquefiable zone and will not affect their capability to absorb demands from an aftershock that is equivalent in ground shaking to the Hosgri mainshock.

Based on the above evaluation of the main ASW bypass components for the assumed aftershock ground motions that are equivalent to those of the Hosgri mainshock, concurrent

with liquefaction effects, PG&E concludes that there would be no adverse impact on the ASW bypass segment in this area at DCPP since all components are within our acceptance criteria (Reference 5c-3).

References

7-1 "Final Report of the Diablo Canyon Long Term Seismic Program," prepared by PG&E, dated July 1988.

7-2 Jones, L. M., R. Console, F. Di Luccio, and M. Murru, 1995: "Are foreshocks mainshocks whose aftershocks happen to be big? Evidence from California and Italy," EOS, Transactions, American Geophysical Union, Vol. 76, No. 46, pp. F388-F389.

7-3 Wells, D., and K. Coppersmith, 1994: "New empirical relationships among magnitude, rupture length, rupture width, rupture area, and surface displacement," Bulletin of the Seismological Society of America, Vol. 84, No. 4, pp. 974-1002.

7-4 PG&E Letter DCL-97-150, License Amendment Request 97-11, "Auxiliary Saltwater System Piping Bypass Unreviewed Safety Question," dated August 26, 1997.

7-5 PG&E Letter DCL 97-091, "Response to Request for Additional Information Concerning Auxiliary Saltwater System Piping Bypass Project - Diablo Canyon Units 1 and 2," dated May 15, 1997.

Question 8

Provide the detailed qualification of the reinforced concrete anchor thrust blocks that may be affected by displacements within the soil liquefaction zone. Include the loading condition associated with simultaneous start-up of all ASW pumps.

PG&E Response to Question 8

Thrust Blocks in Soil Liquefaction Zone

There are three ASW concrete anchor thrust blocks located within the potential liquefiable zone as shown on Reference 8-1. These thrust blocks are supporting the ASW bypass pipes for the two Unit 1 trains. Block TB-4, with an equivalent plan dimension of 9 feet x 16 feet and 8 feet in depth, has Dresser couplings installed at the south and east block surfaces. Block TB-5 has a plan dimension of 11 feet x 14 feet and 6 feet in depth. Block TB-6, with an equivalent plan dimension of 7 feet x 13 feet and 8 feet depth, has Dresser couplings installed at the south block surface. Each concrete anchor thrust block has #6 reinforcing bar at 12 inch spacing around the perimeter of all block faces, which provides moment resisting capability around both the horizontal and vertical axes. Additional diagonal rebars are added to reinforce the block at the piping penetrations.

For cross-referencing purposes, thrust blocks designations TB-4, TB-5, and TB-6 on Reference 8-1 equate to Block D, C2, and C respectively, as shown on Figure 5b-1 of our response of May 15, 1997 (i.e., same as March 25, 1997 response).

Critical Loading Combinations

The critical loading combinations for the thrust blocks located in the soil liquefaction zone are as follows:

$$U = D + T_A + P_A + HE$$

$$U = D + T_A + P_A + LE$$

where

- U = capacity based on the strength design method per ACI 318-71 (Reference 8-2)
- D = dead load associated with the anchor block structural system
- T_A = abnormal thermal load due to the maximum temperature for ASW operating modes per References 5c-1 and 5c-2
- P_A = abnormal internal pressure load: Maximum 102 psi at the ASW pump discharge point for ASW operating modes per References 5c-1 and 5c-2 and

includes simultaneous start-up of all ASW pumps

HE = seismic loads due to Hosgri event

LE = soil liquefaction effect loads due to the vertical displacement at the blocks and piping after a Hosgri event

Thrust Block Demands

The liquefaction effect loading combination (LELC) produces the largest demand for the concrete thrust blocks within the potential liquefiable zone. For the LELC case, the governing demands for the thrust blocks are bending moments about the horizontal axis, from imposed vertical differential displacements associated with soil liquefaction. Concurrent internal piping pressure from ASW pump startup induces an unbalanced thrust load on the concrete blocks due to changes in direction in pipe routing at the thrust block.

Liquefaction induced vertical ground settlement contribute to an additional angular change and hence, added unbalanced thrust load due to internal pressure. This added unbalanced load is deemed insignificant since (1) a 1/2 inch of maximum vertical settlement developed over 25 feet results in a small maximum angular change of less than 0.1 degree with respect to pipe routing directional changes and (2) the resultant of unbalanced thrust load on a concrete block undergoing a vertical settlement is in the downward direction and does not affect the overall block sliding stability.

For the Hosgri loading combination due to seismic horizontal differential ground displacements perpendicular to ASW piping run, the governing demands are primarily bending moment about the vertical axis. These moments act orthogonal to those affected by LELC case.

For the Hosgri loading combination due to seismic horizontal differential ground displacements in the axial direction of ASW piping, the maximum imposed seismic loads are limited by soil friction against the buried ASW pipes. The Hosgri load combination results in the maximum thrust force demand to each thrust block.

Evaluation of Individual Thrust Blocks

Block TB-4 with its associated Dresser couplings at pipe-block interface on both faces, allows the pipe to rotate and move in the axial direction of the pipe, and reduces load demands on the piping, as well as on the thrust block due to imposed seismic loads or the soil liquefaction settlements. As shown in Reference 8-1, this block is located along the boundary of the potential liquefiable soil zone. As a result of ground settlement, Block TB-4 will undergo a "rigid body" rotation conforming to the 1/2 inch over 25 feet slope with negligible moment demand since it is isolated from the piping by the Dresser couplings. Consequently, liquefaction effect on this block is negligible.

Maximum moment demands and capacities associated with Blocks TB-5 and TB-6 for different loading combinations are shown in Table 8-1. Maximum thrust demands and sliding resistance capacities associated with Blocks TB-4 through TB-6 for the Hosgri loading combination are shown in Table 8-2.

Table 8-1

Summary of Thrust Block Moment Demands and Capacities

Hosgri Load Combination

Thrust Block Designation	Moment Demand (k-ft) for Hosgri Load Combination	Moment Capacity (k-ft)
TB-5	508 (V)	1,100
TB-6	417 (H)	1,800

Hosgri-Induced Liquefaction Effect Load Combination

Thrust Block Designation	Moment Demand (k-ft) for LELC	Moment Capacity (k-ft)
TB-5	394 (V)	1,100
TB-6	1,045 (H)	1,800

where H indicates bending about the horizontal axis and V indicates bending about the vertical axis; only governing moment demands are listed.

Table 8-2

Summary of Thrust Demands and Sliding Resistance Capacities

Thrust Block Designation	Thrust Demand (k) for Hosgri Load Combination	Sliding Resistance Capacity (k)
TB-4	121	158
TB-5	73	108
TB-6	215	265

Based on the above evaluation, it is concluded that the anchor thrust blocks in the soil liquefaction zone are able to maintain the system structural and operational integrity under all applicable loadings including the simultaneous start up loads from all ASW pumps.

References

8-1 PG&E Sketch SK-C-4016686, Rev. 0, Potentially Liquefiable Sand Layer Limits Near ASW Bypass Piping.

8-2 ACI 318-71, Building Code Requirements for Reinforced Concrete, by American Concrete Institute.

Question 9

Provide the inservice inspection measures to detect future potential corrosion of the buried piping.

PG&E Response to Question 9

The ASW bypass piping is protected by a Cathodic Protection (CP) system consisting of an impressed current and sacrificial anode systems. In addition, the pipe, now buried above sea level, is coated with two coats of Devguard 238 with a fiberglass lining, and backfilled with clean sand.

The operating portion of the CP system was installed in 1995 and 1996, and presently protects the buried ASW bypass piping near the Intake and on the adjacent hillside.

The CP system is monitored on a regular basis and is included within the scope of PG&E's program for implementing the Maintenance Rule (10 CFR 50.65). Guidance for the monitoring was provided by CC Technologies, who designed and oversaw installation of the system. Maintenance Procedure (MP) E-72.2, "Monthly Cathodic Protection System Monitoring," which provides guidance for monitoring and adjustment of the plant CP sytems, is being revised to incorporate inclusion of the ASW CP system. The revision will be completed by the end of 1997. The procedure will assure that the CP system is operating and providing the required amount of current throughout the system.

Due to the non-corrosive environment, exterior coating, and a CP system, no inservice external corrosion inspection measures are planned.

Reference

9-1 Maintenance Procedure (MP) E-72.2, "Monthly Cathodic Protection System Monitoring."

ATTACHMENT 2-1

Dresser Coupling
24 1/2" O. D. Style 38 Coupling

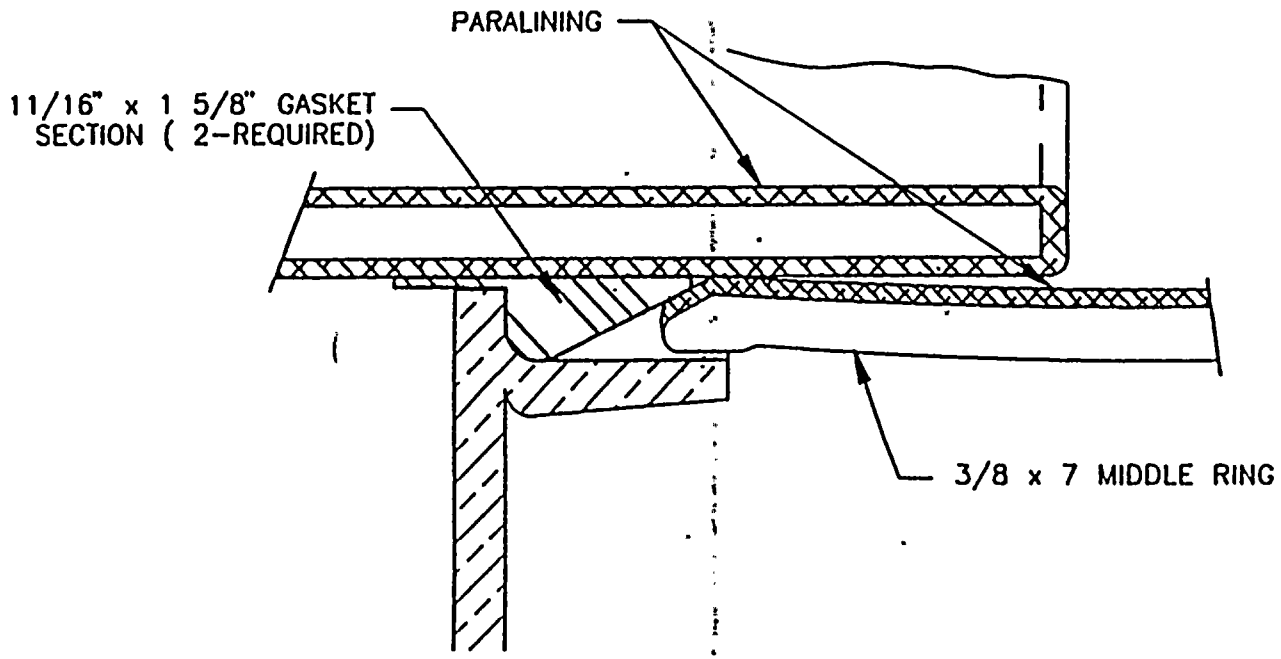

DETAIL (2)

24 1/2" O.D. STYLE 38 COUPLING

(SCALE: 3/4"=1")

ATTACHMENT 2-2

Dresser Couplings Seismic Qualifications, Test Report No. 14333, "Seismic Vibration Testing of One 14" Dresser Style 38 Coupling for Dresser Manufacturing Div. of Dresser Industries, Inc. Under Purchase Order No. 37443," dated November 15, 1978

Dresser Couplings SEISMIC QUALIFICATIONS

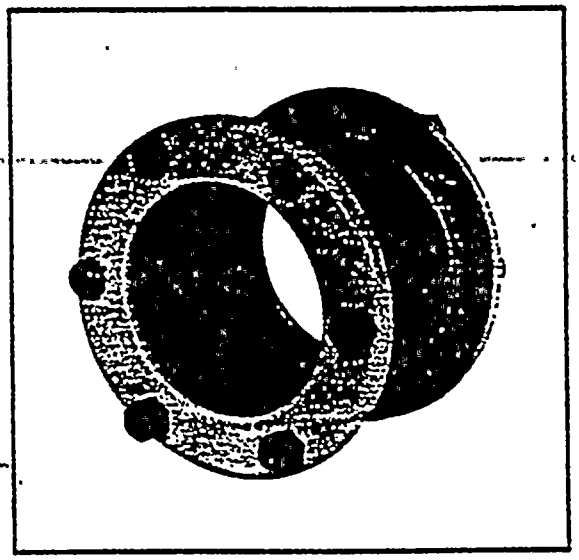

dmd DRESSER

DRESSER MANUFACTURING DIVISION
DRESSER INDUSTRIES INC.
Bradford, Pennsylvania 16701